Pharmaceutical Research, Vol. 7, No. 5, 1990

Research Article

Chemical Stability of Pentostatin (NSC-218321), a Cytotoxic and Immunosuppressant Agent

Laman A. Al-Razzak,[1,2] Annalisa E. Benedetti,[1] Wanda N. Waugh,[1] and Valentino J. Stella[1,3]

Received March 6, 1989; accepted November 6, 1989

Pentostatin, an unusual nucleoside of natural origin, has been used for the treatment of hairy cell leukemia, as an immunosuppressant agent, and as an inhibitor of adenosine deaminase. The studies of the physicochemical properties and solution stability of pentostatin (**1**) are important to the development of a parenteral formulation for extensive preclinical and clinical testing. Pentostatin displayed apparent pK_a values at 25 ± 0.1°C and ionic strength of 0.15 *M* of 2.03 ± 0.03 and 5.57 ± 0.14 (spectrophotometric) and 5.50 ± 0.02 (potentiometric) for N_1 and the amidine nitrogen in the seven-membered ring, respectively, which are the most likely protonation sites. The rates of degradation of pentostatin were determined as a function of pH, buffer concentration, and temperature. In the pH range 1.0–4.0, pentostatin undergoes acid-catalyzed glycosidic cleavage leading to the formation of the base compound, **2**, and 2-deoxyribose. A carbonium ion mechanism in which C–N bond cleavage was the rate-determining step was consistent with the data. In the pH range 6.5–10.5, the imine bond at C_5 position in pentostatin is hydrolyzed to form the corresponding formamide. Pentostatin hydrolysis in this pH range was independent of pH. At pH >11, pentostatin decomposes to nonchromophoric products probably through multiple-step base-catalyzed hydrolytic mechanisms. Pentostatin appears to be quite stable after reconstitution of a lyophilized experimental dosage form. Care must be taken if pentostatin is extensively diluted with 5% dextrose in water, as pentostatin stability is compromised at pH values less than 5.

KEY WORDS: pentostatin; nucleoside; hydrolysis; pK_a; hairy cell leukemia; immunosuppressant; adenosine deaminase inhibitor; stability; formulation.

INTRODUCTION

Pentostatin, (8*R*)-3-(2-deoxy-β-D-erythro-pentofuranosyl)-3,6,7,8-tetrahydroimidazo[4,5-*d*]-[1,3]diazepin-8-ol (**1**) (Fig. 1), is a potent, tight-binding inhibitor for the enzyme adenosine deaminase (1), with a k_i of 2.5×10^{-12} against human erythrocytic adenosine deaminase. Adenosine deaminase is an enzyme responsible for N_6-deamination of adenine nucleosides. Therefore, pentostatin was initially used in combination with other antiviral and antitumor nucleosides, especially ara-A (2), in an attempt to improve their clinical properties. Pentostatin alone has also demonstrated a unique activity as an immunosuppressant (3) by preventing the maturation of lymphocytes.

Pentostatin has an unusual nucleoside structure. It was initially isolated from the fermentation beers of *Streptomyces antibioticus* NRRL 3238 (3). In 1979 Baker and coworkers (4–6) developed a successful total synthesis for pentostatin. The early clinical use of pentostatin was not encouraging, however, it has recently been used in a low dose, 4 mg/m^2, in the treatment of hairy cell leukemia (7). Patients who received treatment showed complete remission, in addition to clearing hairy cells from the bone marrow. Interest in the use of the deaminase inhibitor properties of pentostatin has also increased since many of the newer agents used in the treatment of AIDS are readily deaminated.

For most clinical studies to date, pentostatin has been used in a freeze-dried dosage form containing 10 mg of pentostatin, 50 mg of mannitol, and sodium hydroxide for pH adjustment. Earlier reports, based on a nonspecific uv assay, suggested that pentostatin showed maximum stability in the pH range 7.5–10. The lyophilized produce was reconstituted with 0.9% sodium chloride injection USP (NS), prior to administration. Due to the lack of good quantitative data on the chemical stability of pentostatin *per se* and the stability of preclinical and clinical freeze-dried reconstituted samples, studies were undertaken to provide up-to-date information on the physicochemical properties of this compound, including its solution stability at various pH values, buffer concentrations, and temperatures as well as isolation and structural elucidation of the degradation products. The results of these preformulation studies are presented here.

MATERIALS AND METHODS

Pentostatin (NSC-218321) was supplied by the National

[1] Department of Pharmaceutical Chemistry, School of Pharmacy, University of Kansas, Lawrence, Kansas 66045.
[2] Current address: Abbott Laboratories, Pharmaceutical Products Division, Department 493, North Chicago, Illinois 60064.
[3] To whom correspondence should be addressed.

0724-8741/90/0500-0452$06.00/0

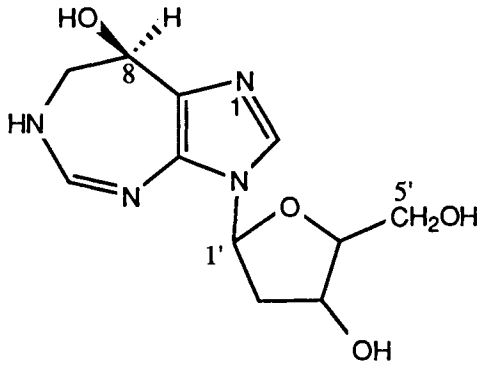

Fig. 1. Pentostatin.

Cancer Institute, Bethesda, MD (Lot 20133 × 46B), through the supplier Warner–Lambert. All other chemicals including buffer components were reagent grade obtained from commercial sources and were used without further purification. All organic solvents were HPLC grade. Aqueous solutions and buffers were prepared with deionized and glass-distilled water (Mega-Pure System, Model MP-1, Corning). All pH measurements were conducted at 25°C with a digital pH meter, Corning Model 155 (Medfield, MA). Proton and ^{13}C NMR spectroscopy were measured at 300 MHz with a Varian XL-300 spectrometer using deuterium oxide as a solvent (Aldrich, 99%). Chemical shifts (δ ppm) are reported for band centers relative to deuterium oxide (δ 4.67 ppm) in ^{1}H NMR and relative to an internal standard, sodium 3′-trimethylsilyl propionate (TSP; δ = 0.00 ppm), in ^{13}C NMR. Ultraviolet spectra were measured with a Shimadzu-260 recording spectrophotometer. Mass spectra were obtained from a Varian CH_5 or Ribermg R-10-10 quadrapole mass spectrometer or performed at Midwest Center for Mass Spectrometery (University of Nebraska, Lincoln).

High-performance liquid chromatography (HPLC) was performed using a system consisting of a Kratos Spectroflow 400 solvent delivery system linked to a Kratos spectroflow 480 injector fitted with a 20-μl loop. The detector was a variable-wavelength Kratos spectroflow 783 operated at 280 nm and peak areas were determined by a Nelson Analytical integrator. The HPLC studies were conducted using a reverse-phase C_{18} (Shandon 150 mm × 4.6-mm ODS Hypersil, 5 μM) column. The mobile phase contained 2.5 parts methanol with 97.5 parts 0.01 *M* phosphate buffer, pH 7.0, and the flow rate was 2 ml/min. Retention volume for pentostatin was 15.4 ml. The major acidic degradation product, 2, had a retention volume of 2.96 ml, while 3, the major alkaline degradation product, had a retention volume of 9.60 ml. In the alkaline region (pH >10.0) degradation products which eluted at the solvent front could be detected at 204 nm but not at 280 nm. Calibration curves of 0.003–0.04 mg/ml 1 were constructed from linear plots of peak area versus concentration.

Isolation of the Acidic Degradation Products. One hundred milligrams of pentostatin was dissolved in 50 ml of aqueous hydrochloric acid solution at pH 1.0. The hydrolysis reaction was followed to completion by HPLC (defined as complete disappearance of the pentostatin). The solvent was evaporated *in vacuo* and the residue was used for characterization. The residue showed a single uv absorbing peak on the HPLC. Since the products from the hydrolysis were difficult to isolate and crystallize, the products were characterized without actual isolation by comparing the NMRs of the degraded sample to the parent molecule and the known NMR properties of 2-deoxyribose. The acidic degradation products were characterized as 2, (8*R*)-3,6,7,8-tetrahydroimidazo [4,5-*d*]-[1,3]diazepin-8-ol (the base of the nucleoside pentostatin) resulting from cleavage of the glycosidic linkage, and 2′-deoxyribose. The reaction can be seen in Fig. 2. The ^{1}H NMR (D_2O) for 2 and 2-deoxyribose mixture data are δ 1.5–1.92 (m, 2H, $C_{2'}$); δ 3.62 (m, 4H, $C_{5'}$, $C_{4'}$, $C_{3'}$); δ 5.136–5.19 (t, 1H, $C_{1'}$); δ 7.647 (s, 1H, C_5); δ 7.852 (s, 1H, C_2). The ^{13}C NMR data in D_2O for 2 and 2′-deoxyribose are δ 33.72, 35.10 (C2′); δ 48.97 ($C_{7'}$); δ 61.80, 66.54 ($C_{5'}$); δ 62.88 (C_8); δ 64.60, 66.54 ($C_{3'}$); δ 67.33, 67.50 ($C_{4'}$), δ 91.70, 93.91($C_{1'}$); δ 133.10 (C_5). The chemical ionization mass spectrum of the decomposition mixture showed a molecular ion m/e of 153 corresponding to 2 and 134 for 2′-deoxyribose.

Isolation of the Neutral Degradation Product 3. A solution of 100 mg pentostatin (0.373 mmol) in 100 ml 0.01 *M* phosphate buffer at pH 7.0 was allowed to reflux for 10 hr. The reaction was monitored by HPLC and the reaction was stopped when HPLC analysis showed peak areas of 80% for pentostatin and 15% for the major degradation product. The solvent was removed *in vacuo* and the reddish-brown residue was redissolved in 10 ml of water. The solution was then filtered through a 0.2-μm disposable filter assembly (Acrol 93). Compound 3 was then isolated by passage twice through a preparative HPLC system using a Whatman column (Partisil 10 PDS-2, 50 cm × 9.4-mm i.d.). The mobile phase used was 2.5% methanol in 0.01 *M* ammonium formate buffer at a flow rate of 3 ml/min with an injection volume of 2 ml. Ultraviolet detection was used at 280 nm to follow the separation of 3 from pentostatin and other minor components. The pure product was freeze-dried using a Virtis bench top freeze dryer, Model 1.5. ^{1}H NMR (D_2O) data for 3 are δ 2.37 (m, 2H, $C_{2'}$); δ 3.206 (m, 2H, C_7); δ 3.614 (m, 2H, $C_{5'}$); δ 3.914 (q, 1H, $C_{4'}$); δ 4.38 (m, 1H, $C_{3'}$); δ 4.723 (d, 1H, C_8); δ 5.838 (t, 1H, $C_{1'}$); δ 7.874 (s, 1H, C_2); δ 8.282 (s, 1H, NCO-H). The chemical ionization mass spectrum for 3 displayed a molecular ion peak m/e of 287 corresponding to the molecular weight for 3 + 1.

pK_a Determination. The pK_a values of pentostatin were determined using uv spectroscopy and by potentiometric titration (8). For the spectroscopic method a 100-μl aliquot of a 1.5×10^{-3} *M* solution of pentostatin in water was diluted with 1.0 ml of 0.05 *M* buffer solution (μ = 0.15 with NaCl) at various pH values (pH range, 1.0–8.0). Samples of the resulting solutions were placed into a cuvette thermostated at 25°C. The changes in the absorbance were monitored at 279 and at 300 nm for the determination of pK_{a1} and pK_{a2}, respectively. Sodium hydroxide solution (0.1 *N*) was used to determine the absorbance of the neutral pentostatin at high pH, and 1.0 *N* hydrochloric acid solution was used to determine the absorbance of the fully diprotonated pentostatin. At low pH solutions (pH <3.0) it was necessary to extrapolate the absorbance measurement to zero time since pentostatin ready undergoes degradation under acidic conditions. The lower pK_a was also determined at zero buffer concentration with no ionic strength adjustment by measuring the pK_a at three different buffer concentrations (0.01,

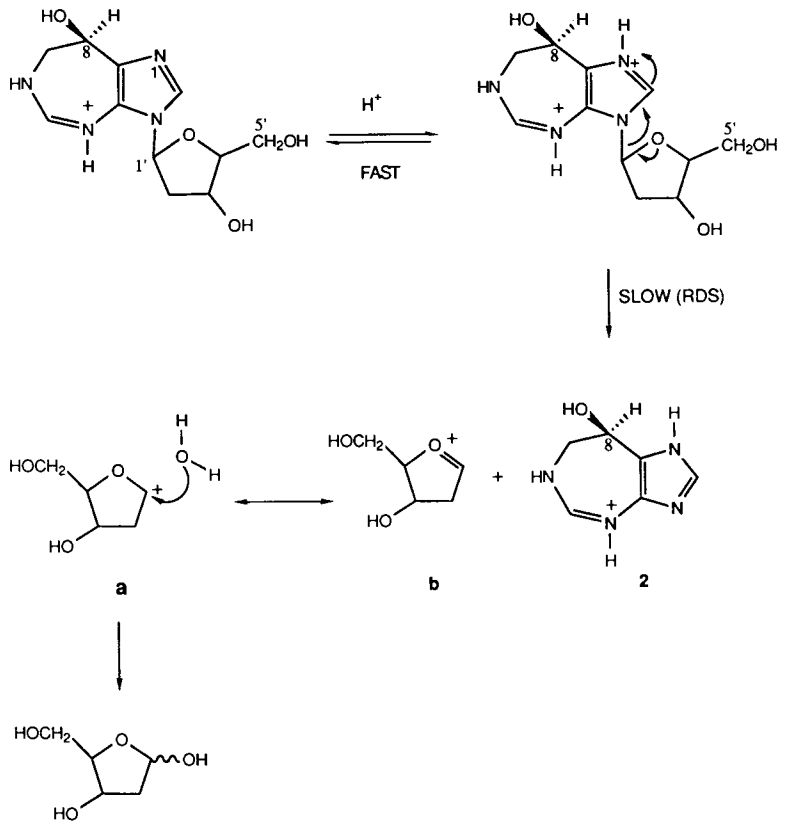

Fig. 2. Proposed mechanism for acid-catalyzed hydrolysis of pentostatin (pH <5.0).

0.1, and 0.5 *M*) and extrapolating to zero buffer (and ionic strength) concentration (8). For potentiometric titration a pentostatin solution (0.1 *M*, initial pH ≈8) containing 0.15 *M* NaCl was prepared using glass-distilled water and thermostated at 25°C. The resulting solution was titrated with standardized 0.1 *N* HCl solution. After each addition, 1 min was allowed for mixing prior to pH reading.

Kinetic Studies. Degradation of pentostatin was studied over a pH range of 1.0–12.7 at 25.0 ± 0.1°C. For these studies, a weighed quantity of drug was dissolved in buffer to give a final concentration of approximately 1.1×10^{-4} *M*. Buffers were used at varied concentrations, keeping the ionic strength constant at 0.15 *M* (NaCl). Systems employed were 0.1 *N* hydrochloric acid (pH 1.0); 0.01 *N* hydrochloric acid (pH 2.0); 0.025, 0.05, 0.075 *M* formate (pH 3.0–4.0); 0.025, 0.05, 0.075 *M* acetate (pH 5.0); 0.025, 0.05, 0.075 *M* phosphate (pH 6.0–7.5); 0.05 *M* carbonate (pH 9.82–10.5); 0.01 *N* sodium hydroxide (pH 11.78); and 0.1 *N* NaOH (pH 12.71). Samples were stored in water baths at 25.0°C and aliquots were removed at appropriate intervals for analysis by HPLC. When the hydrolytic reaction was very fast (pH <3.0), samples were withdrawn at very short time intervals and the reaction was quenched by adding 0.1 *M* phosphate buffer at pH 7.0 and refrigerated. In the HPLC analysis both disappearance of reactant and appearance of compound 2 or 3a (Figs. 2 and 3) were monitored. Observed first-order rate constants were calculated from the slope of linear plots of log *C* versus time, where *C* is the concentration of the remaining intact pentostatin. When buffer catalysis was observed, the apparent first-order rate constants at zero buffer concentration were extrapolated from linear plots of k_{obs} versus buffer concentration. Studies of the stability of pentostatin at pH 3.0 and pH 7.0 at various temperatures (37, 30, 25, and 15°C at pH 3.0; 70, 50, 37, and 25°C at pH 7.0) were conducted to determine the energy and the entropy of activation. The pH values were standardized at the temperatures of reaction. The influence of ionic strength on the rate of hydrolysis of pentostatin in 0.01 *M* phosphate buffer, pH 7.0, at 25°C was studied using solutions with μ = 0.03, 0.05, 0.07, 0.09, 0.11, 0.13, and 0.15 *M* (NaCl). The solvent deuterium isotope effect on the hydrolysis of pentostatin was studied using 0.03 mg/ml of pentostatin in 0.01 *M* phosphate buffer (pH or pD = 7.4) prepared in 100% H_2O, 50% D_2O, and 100% D_2O at an ionic strength of 0.03 (NaCl).

Stability of the Lyophilized Pentostatin Formulation Reconstituted and Diluted with iv Fluids. The lyophilized formulations of pentostatin were prepared by Ben Venue Laboratories, Lot BV-87-720. Each bottle contained 10 mg of pentostatin, 50 mg of mannitol, and sodium hydroxide to adjust pH. All of the samples were reconstituted with 5.0 ml of normal saline (NS) as per directed on the label. Dilutions were made by injecting the total reconstituted sample into a nominal 500-ml container of either NS or 5% dextrose in water (D5W) for a final concentration of, nominally, 2×10^{-2} mg/ml of drug. Dilutions containing nominally 2×10^{-3} mg/ml of drug were prepared by injecting a 0.5-ml aliquot (by syringe) of the reconstituted sample into nominal 500-ml containers of either NS or D5W. The NS and D5W were supplied in both glass bottles and PVC infusion bags. All concentrations of drug in each iv fluid in each type of con-

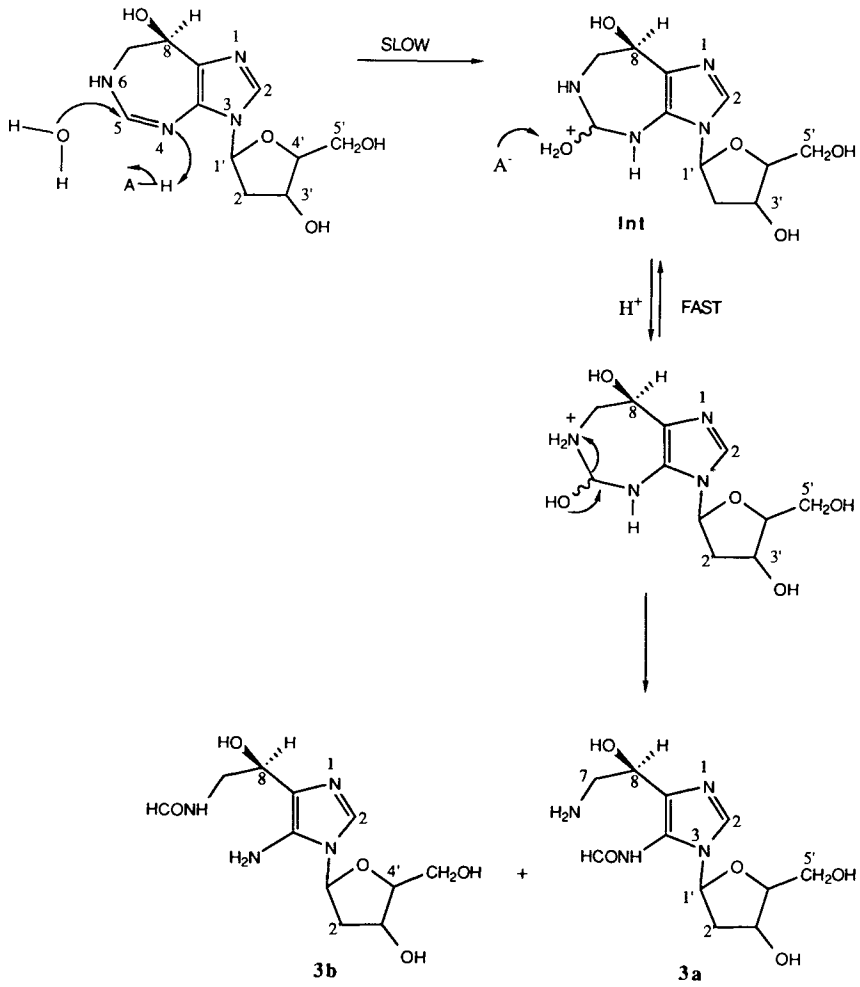

Fig. 3. Proposed mechanism for pentostatin hydrolysis to 3a in neutral aqueous solutions.

tainer were analyzed in duplicate. Concentrations were close to the nominal values even though no allowance was made for the fact that the iv fluid containers usually contain an average and not an exact 500 ml. In most cases the concentration of drug is less than the theoretical for one vial (10 mg) per 500 ml or 0.5 ml (1 mg) per 500 ml. All of the dilutions were stored at ambient temperature (22–23°C). The solutions were analyzed for intact drug over a 48- to 72-hr period of time using our stability-indicating HPLC procedure.

RESULTS AND DISCUSSION

The apparent pK_a values for pentostatin in H_2O, uncorrected for activity coefficients, were determined by spectrophotometric and potentiometric titration methods. pK_{a1} was determined spectrophotometrically and found to be 2.03 ± 0.03 [using 0.05 *M* buffers and an ionic strength of 0.15 (NaCl)]; extrapolation to zero buffer (and ionic strength) concentration gave a value of 1.67 ± 0.03. The second pK_a was measured both spectrophotometrically, 5.57 ± 0.14, and potentiometrically, 5.50 ± 0.02, at an ionic strength of 0.15 (NaCl). The sites of protonation have been assigned to N_1 and the amidine nitrogen in the seven-membered ring of the nucleoside for pK_{a1} and pK_{a2}, respectively. These values are consistent with literature values for similar compounds (9,10).

Hydrolysis of Pentostatin. The hydrolysis of pentostatin in aqueous buffered solutions was monitored as a function of pH, buffer concentration, and temperature. The kinetic data contained (one experiment per condition) are shown in Table I. The first-order rate constants, determined at various buffer concentrations with ionic strength held constant at 0.15 with NaCl, were obtained from a plot of log *C* versus time, where *C* is the concentration of pentostatin remaining. In the pH range 1.0–3.0 the acidic degradation product 2 is the only product observed on the HPLC chromotograms. Due to the lack of uv absorbance, 2-deoxyribose was not observed except by NMR and mass spectrometry of the reaction mixture. No catalysis by buffers was observed in this pH range. The absence of general acid–base catalysis by formate buffers has been reported previously in the solvolysis of similar nucleosides (11–13). The major degradation in the neutral to basic pH region was cleavage of the amidine bond in the base portion of pentostatin.

The pH–degradation rate constant data from Table I are plotted in Fig. 4. In those cases where general acid/base

Table I. Apparent First-Order Rate Constants for the Degradation of Pentostatin in Aqueous Solution at 25°C, μ = 0.15

Buffer	Initial pH	k_{obs} (min^{-1})	t_{50} (min)	r
HCl (0.1 *N*)	1.0	1.24×10^{-1}	5.59	0.999
HCl (0.01 *N*)	2.0	0.54×10^{-1}	12.83	0.999
	3.0	8.97×10^{-3}	77.23	—[a]
Formate (0.025 *M*)	3.0	8.92×10^{-3}	77.7	0.999
Formate (0.050 *M*)	3.0	9.00×10^{-3}	77.0	1.000
Formate (0.075 *M*)	3.0	9.00×10^{-3}	77.0	0.999
Formate (0.050 *M*)	4.0	8.33×10^{-4}	8.316×10^{2}	0.999
	5.0	1.24×10^{-4}	5.587×10^{3}	—[a]
Acetate (0.025 *M*)	5.0	1.20×10^{-4}	5.804×10^{3}	0.999
Acetate (0.050 *M*)	5.0	1.28×10^{-4}	5.394×10^{3}	0.999
Acetate (0.075 *M*)	5.0	1.25×10^{-4}	5.563×10^{3}	0.999
	6.0	1.28×10^{-5}	5.414×10^{4}	—[a]
Phosphate (0.025 *M*)	6.0	1.68×10^{-5}	4.125×10^{4}	0.999
Phosphate (0.050 *M*)	6.0	2.19×10^{-5}	3.164×10^{4}	0.997
Phosphate (0.075 *M*)	6.0	2.53×10^{-5}	2.739×10^{4}	0.99
	6.5	8.54×10^{-6}	8.153×10^{4}	—[a]
Phosphate (0.025 *M*)	6.5	1.29×10^{-5}	5.372×10^{4}	0.999
Phosphate (0.050 *M*)	6.5	1.60×10^{-5}	4.331×10^{4}	0.999
Phosphate (0.075 *M*)	6.5	2.10×10^{-5}	3.300×10^{4}	0.999
	7.0	6.99×10^{-6}	1.004×10^{5}	—[a]
Phosphate (0.025 *M*)	7.0	9.31×10^{-6}	7.452×10^{4}	0.999
Phosphate (0.050 *M*)	7.0	1.13×10^{-5}	6.132×10^{4}	0.999
Phosphate (0.075 *M*)	7.0	1.38×10^{-5}	5.033×10^{4}	0.999
	7.5	5.84×10^{-6}	1.195×10^{5}	—[a]
Phosphate (0.025 *M*)	7.5	7.21×10^{-6}	9.612×10^{4}	0.999
Phosphate (0.050 *M*)	7.5	8.00×10^{-6}	8.659×10^{4}	0.998
Phosphate (0.075 *M*)	7.5	9.66×10^{-6}	7.172×10^{4}	0.996
Carbonate (0.050 *M*)	9.8	6.22×10^{-6}	1.118×10^{5}	0.998
Carbonate (0.050 *M*)	10.5	6.30×10^{-6}	1.100×10^{5}	0.998
NaOH (0.010 *N*)	11.8	7.39×10^{-6}	9.376×10^{4}	0.995
NaOH (0.100 *N*)	12.7	1.06×10^{-5}	6.551×10^{4}	0.995

[a] Obtained by extrapolation to zero buffer concentration.

catalysis was observed, the value for k_{obs} was that extrapolated to zero buffer concentration. The observed first-order rate constants for the degradation of pentostatin were analyed according to Eq. (1),

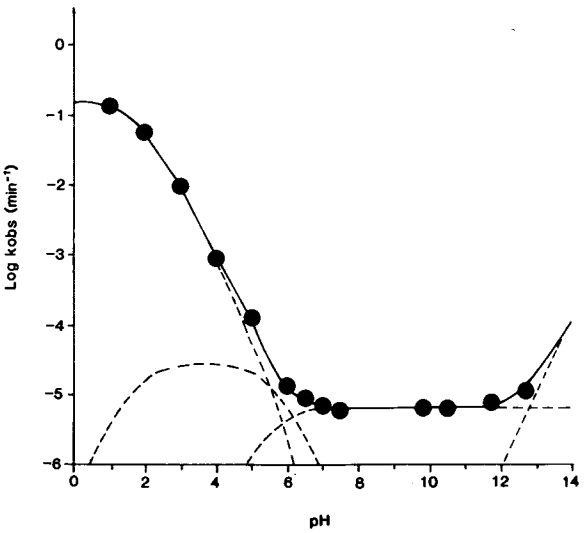

Fig. 4. pH–rate profile for the degradation of pentostatin at 25°C and ionic strength of 0.15 *M* (NaCl). The solid line is that described by Eq. (1), while the dashed lines show the contribution of each term in Eq. (1) to the overall pH-rate profile.

$$k_{obs} = k_H[H^+]f_{PH^+} + k'_H[H^+]f_P + k'_o f_P + k'_{OH}[OH^-]f_P \quad (1)$$

where $f_{PH^+} = [H^+]K_{a1}/([H^+]^2 + [H^+]K_{a1} + K_{a1}K_{a2})$ is the fraction of pentostatin in the monoprotonated form, and k_H is the bimolecular rate constant for hydrogen ion-catalyzed hydrolysis of the monoprotonated pentostatin (PH^+). The first term in Eq. (1) is kinetically equivalent to the spontaneous breakdown of the diprotonated pentostatin. As discussed later, the latter process may be the more likely mechanism for the breakdown of pentostatin at pH values <5.

The rate constant, k_H, was determined by plotting the inverse of k_{obs} versus the inverse of hydrogen ion for the data between pH values 1.0 and 3.0. In this pH range, k_{obs} can be described by Eq. (2) ($[H^+] \gg K_{a2}$).

$$k_{obs} = k_H[H^+]K_{a1}/([H^+] + K_{a1}) \quad (2)$$

The slope ($1/k_H$) and intercept ($1/k_HK_{a1}$) of the inverse plot yields values of 9.6 M^{-1} min^{-1} for k_H and 1.38×10^{-2} for K_{a1}, corresponding to a pK_{a1} of 1.86, which is in close agreement with the spectrophotometrically determined value of 2.03 ± 0.03.

The term k'_H represents the acid-catalyzed hydrolysis of neutral pentostatin species. The contribution of this term to the pH–rate profile is significant only in the pH range 5–7. Its method of estimation is discussed later. This term $k'_H[H^+]f_P$ is kinetically equivalent to $k_o f_{PH^+}$, i.e., the spontaneous hydrolysis of monoprotonated pentostatin.

The term k'_o is the pH-independent hydrolysis rate constant operating on the neutral species, *P*, where $f_P = K_{a1}K_{a2}/([H^+]^2 + [H^+]K_{a1} + K_{a1}K_{a2})$ is the fraction of pentostatin in the neutral form. The constant k_o was determined from the observed rate constants in the pH range 7.0–10.5, where f_P is essentially equal to one and this term numerically dominated the profile. The term $k'_o f_P$ is kinetically equivalent to hydroxide-catalyzed hydrolysis of the monoprotonated pentostatin, $k_{OH}[OH^-]f_{PH^+}$, where k_{OH} is the rate constant for the alkaline-catalyzed hydrolysis of the fraction

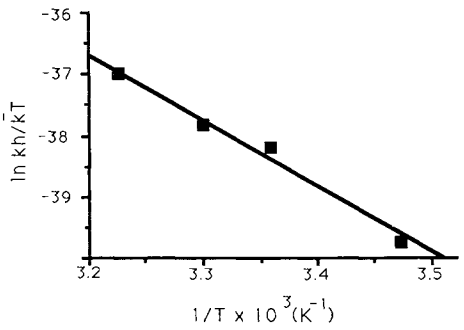

Fig. 5. Eyring plot for the hydrolysis of pentostatin at pH 3.0.

of pentostatin present in its monoprotonated form. Mechanistically, as discussed, below, it appears that water attack on the neutral pentostatin reasonably describes the hydrolysis of pentostatin in this pH range. The term k'_{OH} is the hydroxide-catalyzed hydrolysis rate constant operating on *P*. This rate constant was determined from the slope of the observed rate constant versus the hydroxide ion concentration in the pH range 10.5–12.7, which also assumes that f_p is approximately one.

When only the first, third, and fourth terms in Eq. (1) were used to generate a calculated pH–rate profile, a significant deviation between the observed data and the calculated line was noted in the pH region, 5–7. Using values of 1.38×10^{-2} for K_{a1} and 3.16×10^{-6} for K_{a2}, a manual iterative method was used to estimate the contribution of k'_H to the profile. The solid line (Fig. 4) was drawn using values of 9.6 M^{-1} min^{-1} for k_H, 8.7 M^{-1} for k'_H, 6.25×10^{-6} min^{-1} for k'_O, 1.25×10^{-4} M^{-1} for k'_{OH}, 1.38×10^{-2} for K_{a1}, and 3.16×10^{-6} for K_{a2}. The numerical similarity between k_H and k'_H probably accounts for the fact that the pH–rate profile does not undergo a major perturbation around pK_{a2}.

Pentostatin showed greater instability under acidic compared to alkaline conditions. At pH 1.0 the $t_{1/2}$ of pentostatin was 5.6 min. The major reaction appeared to be the glycosidic cleavage to give 2 and 2-deoxyribose (Fig. 2). The proposed structure of 2 was confirmed by ^{1}H and ^{13}C NMR data. ^{1}H and ^{13}C NMR literature data of 2-deoxyribose (α, β) indicated that the sugar can exist in aqueous solution in the pyranose or furanose form (14). By comparing our data to the literature (15, 16), it was concluded that 2-deoxyribose existed mainly in the pyranose form. In chemical ionization mass spectrometry, 2 showed a molecular ion m/e of 153, while 2′-deoxyribose gave a molecular ion m/e 134.

A mechanistic explanation of the acid solvolysis of pentostatin to 2 and 2-deoxyribose can be proposed based on the solvolysis of similar nucleosides (9,10). The solvolysis of pentostatin probably occurs via rate-limiting unimolecular rupture of the *N*-glycosyl bond of the diprotonated pentostatin species. The alternative mechanism for the glycosidic linkage solvolysis involving the sugar ring opening to form a Schiff base intermediate is considered unlikely (17) in pentostatin hydrolysis. The lack of general acid–base catalysis in formate buffer at pH 3 and acetate buffer at pH 4 and 5 is consistent with the unimolecular mechanism (A-1) for the glycosidic linkage cleavage. It has been shown in the acid-

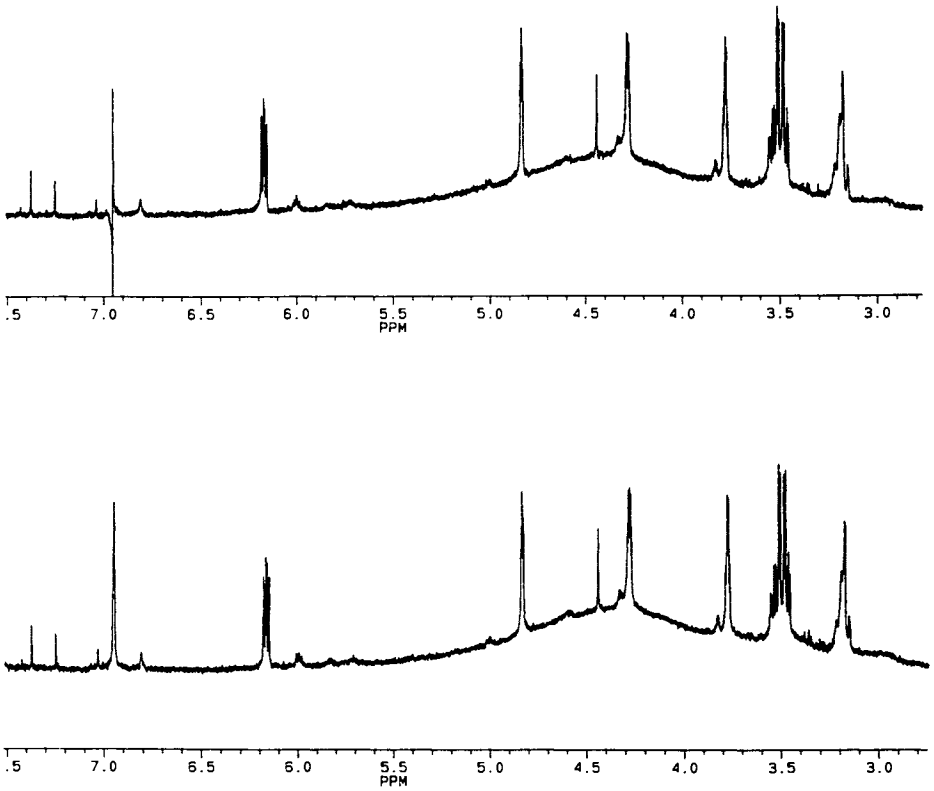

Fig. 6. Partial ^{1}H NMR spectrum (top) of **3a** after irradiation of the amide proton showing that irradiation had no effect on the coupling constant of the C_7 protons at 3.2 ppm and the partial ^{1}H NMR spectrum (bottom) of **3a**.

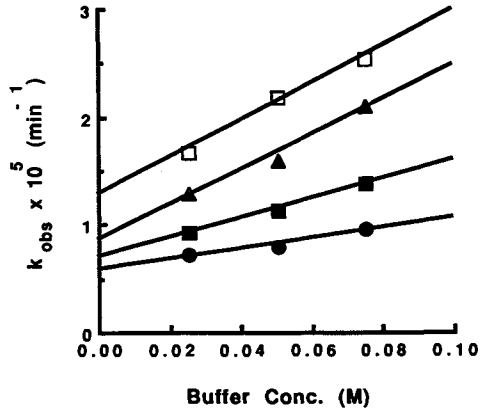

Fig. 7. Dependence of the apparent first-order rate constants on phosphate buffer concentration for the hydrolysis of pentostatin at pH 6.0 (□), 6.5 (▲), 7.0 (■), and 7.5 (●).

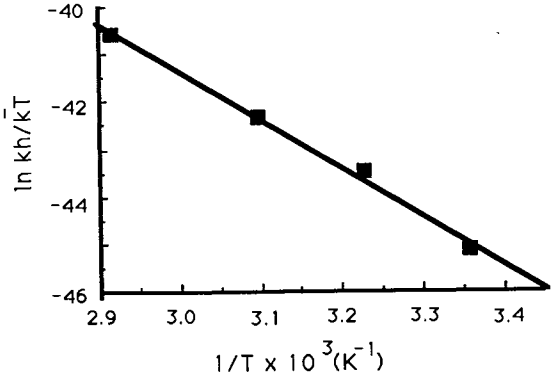

Fig. 9. Eyring plot for pentostatin hydrolysis at pH 7.0.

catalyzed hydrolysis of some purine nucleosides that the mono- as well as the diprotonated nucleosides undergo hydrolysis. The hydrolysis reaction takes place by the same mechanism, differing in the degree of protonation (18,19). The nucleosides hydrolyze first by undergoing a reversible protonation of the purine ring, followed by rate-determining fragmentation to give the purine and a cyclic carboxonium ion form of the sugar. This cation, on reaction with water, gives the 2-deoxyribose (Fig. 2).

The enthalpy of activation, $\Delta H‡$ (21.7 ± 0.6 kcal/mole) and entropy of activation, $\Delta S‡$ (−3.4 ± 3.1 e.u.) for the hydrolysis of pentostatin at pH 3.0 was derived from an Eyring plot (Fig. 5) determined at pH 3.0 at various temperatures (15.0, 25.0, 30.0, and 37.0°C), while an E_a of 22.4 ± 0.9 kcal/mol was determined from an Arrhenius plot of the data. The probability of an A-1 mechanism for solvolysis of the diprotonated pentostatin is favored by the fact that the entropy of activation, $\Delta S‡$, is close to zero.

In the pH range 6.5–9.0, the major decomposition product of **1** was **3**. Compund **3** results from the nucleophilic attack of a water molecule on **1** at the C_5 position. Attack would lead to the intermediate Int (Fig. 3), which then undergoes rapid ring opening to give **3**. There are two possible structural isometric forms of **3**, **3a** and **3b**. Chemical ionization mass spectrometry showed a molecular ion m/e = 287 for **3**, which is the molecular weight of 3 + 1. The fragmentation pattern was consistent with the structure of compound **3**, however, it was not a useful tool to differentiate between the two isomers.

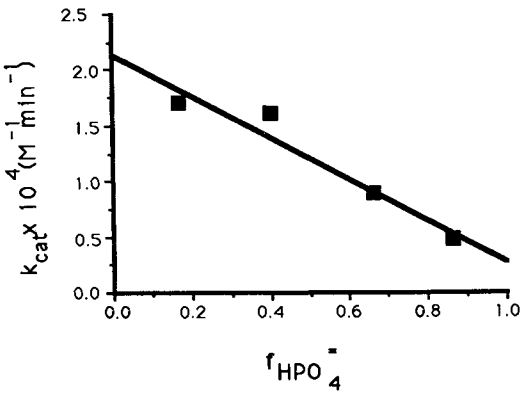

Fig. 8. Dependence of catalytic rates of pentostatin hydrolysis on fraction of phosphate in its dianionic form.

^{1}H NMR data for **3** shows a singlet at δ 8.28 ppm, which was assigned to the formamide proton. Based on literature (20) values, an aromatic formamide has δ values of 8.2–8.7 ppm for the formate proton (*H*CONH-R), while for the aliphatic formamides, δ values of 8.1 ppm have been observed. This difference was considered to be too small to differentiate between **3a** and **3b**. The protons in the ^{1}H NMR of C_2 in **3** are shifted downfield (δ = 7.87 ppm) compared to the parent compound (δ = 7.52 ppm). The two protons at C_7 in compound **1** are chemically nonequivalent, the proton *cis* to the OH group on the adjacent carbon shows an ABC coupling system with J = 4.2 Hz, while the proton *trans* to the OH groups shows a doublet of a doublet with an ABX coupling system (J = 34.8, 12.6 Hz). These two protons are chemically equivalent in **3** due to the free rotation around the C_7–C_8 single bond as a result of ring opening. In compound **3**, the C_1' proton is shifted upfield (δ = 5.838 ppm) compared to the parent compound (δ = 6.06 ppm). The rest of the spectrum was similar for **1** and **3**. The ^{1}H NMR data were useful but not conclusive in differentiating between **3a** and **3b**. However, the decoupling experiment was a more powerful tool to differentiate between the two isomers. Irradiation of the amide proton obtained from ring opening resulted in no effect on the coupling constant of the C_7 protons at 3.2 ppm, which is consistent with **3a** as the product (Fig. 6).

Ultraviolet spectroscopy for compound **3** gave a spectrum very similar to that of the parent compound in acidic, neutral, and alkaline aqueous solutions. This result suggested that both compound **1** and compound **3** have the same

Table II. Stability of Pentostatin in Aqueous Acidic Solutions at 37.0 ± 0.1°C

pH	t_{90} (min) (exp)	t_{50} (min) (exp)	t_{50} (min) (calc)[a]	r
1.0	0.198	1.28	1.32	0.997
2.0	0.52	3.46	3.16	0.998
3.0	3.2	21.0	19.0	0.998
3.5	10.5	69.3	62.1	1.0

[a] Based on pH–rate profile.

Table III. Percentage of Pentostatin Remaining at Various Times After Reconstitution and Dilution of Clinical Samples with iv Fluids Stored at Ambient Temperature

Diluent	Drug conc. ± SD (mg/ml)	Container	Initial pH	Time (hr)	Final pH	% Initial drug remaining	Est. t_{90} (hr)
NS	2.08 ± 1.9%	Reconstituted as received	7.74 ± 0.06	72	7.23 ± 0.01	97.1 ± 0.7	>72
D5W	1.90×10^{-2} ± 0.7%	Glass[a]	5.74 ± 0.01	50	5.42 ± 0.06	91.8 ± 1.9	54
	2.02×10^{-3} ± 1.7%	Glass[a]	4.74 ± 0.06	51	4.64 ± 0.07	62.3 ± 0.7	11
	1.86×10^{-2} ± 4.4%	PVC[b]	5.36 ± 0.09	51	5.28 ± 0.02	88.4 ± 0.8	45
	1.93×10^{-3} ± 0%	PVC[b]	4.59 ± 0.01	51	4.58 ± 0.06	60.9 ± 1.8	11
NS	2.02×10^{-2} ± 1.7%	Glass[c]	6.35 ± 0.01	49	6.35 ± 0.01	96.3 ± 0.3	>49
	2.04×10^{-3} ± 0.7%	Glass[c]	6.04 ± 0.01	48	6.07 ± 0.02	96.8 ± 1.0	>48
	1.85×10^{-2} ± 0.4%	PVC[d]	6.20 ± 0.12	50	6.17 ± 0.12	99.2 ± 0.4	>50
	1.98×10^{-3} ± 0.4%	PVC[d]	5.71 ± 0.02	48	5.72 ± 0.05	93.7 ± 1.0	>48

[a] Travenol; glass, 500 ml; Lot G786061.
[b] Baxter; PVC bag, 500 ml; Lot C077560.
[c] Abbott; glass, 500 ml; Lot 06-116-DM-02.
[d] Travenol; PVC bag, 500 ml; Lot C076125.

chromophore, which is more consistent with **3a** as the correct isomeric form. The pK_a of **3** was determined spectrophotometrically to be approximately 2.0 at 0.15 ionic strength (NaCl), which is very close to the pK_{a1} value of the starting material. Insufficient **3a** was isolated to allow a potentiometric pK_a to be determined. Mechanistically, intermediate *Int* (Fig. 3) could undergo protonation at either N_4 or N_6. However, since N_6 is more basic than N_4, i.e., it is easier to protonate N_6 compared to N_4, ring opening is more likely to lead to **3a** rather than **3b**. The spectrophotometric, pK_a, and NMR decoupling experiment data are consistent with the fact that the compound exists in the **3a** isomeric form.

In the presence of phosphate buffer (pH 6.0–7.5), pentostatin was subjected to buffer catalysis. Plots of k_{obs} versus total buffer concentration (B_T) were linear. Slopes of the buffer catalysis plots decreased with increasing pH (Fig. 7). By plotting the slopes of the buffer catalysis plots versus the fraction of phosphate in its dianionic form, $HPO_4^=$, it was concluded that catalysis was occurring by both $HPO_4^=$ and $H_2PO_4^-$. However, $H_2PO_4^-$ showed stronger catalysis (Fig. 8) than $HPO_4^=$. This suggests that in this pH range, where the principal reaction appears to be water attack on the C_5 position in the seven-membered ring with concomitant ring opening (Fig. 3), the reaction was subject to general acid catalysis by $H_2PO_4^-$.

The hydrolysis of pentostatin in the neutral range (pH 6.0–8.0) was insensitive to the ionic strength of the reaction solution. The entropy of activation $\Delta S‡$, −21.3 ± 3.2 e.u. (from Fig. 9), derived from the rate of hydrolysis of pentostatin in 0.05 *M* phosphate buffer, pH 7.0, at different temperature was consistent with charge distribution in the transition state. The enthalpy of reaction, from the slope of the Eyring plot, at pH 7.0 was 20.3 ± 1.1 kcal/mol, while E_a, from the slope of an Arrhenius plot of the data, was 20.5 ± 0.5 kcal/mol. Both values are consistent with a hydrolytic mechanism operating in this pH range. The solvent isotope effect study showed a ratio of $k_{H_2O}/k_{D_2O} = 1.1$. These pieces of evidence, especially the lack of an ionic strength effect and a negligible solvent isotope effect, are consistent with the mechanism proposed by DeWolfe (21,22) for the hydrolysis of *N,N'*-diphenylformamidine. This mechanism is based on the free base, and not the conjugated acid undergoing hydrolysis, and the attack of water molecule on pentostatin catalyzed by the general acid being the rate-determining step (Fig. 3).

At pH 5.0, both **2** and **3** were formed, with **2** as the major product. At pH values between 5 and 6, **3a** was the major product, while in the pH range 6.5–9.0, **3a** was the only product observed by HPLC. Compound **3a** is not stable in alkaline solutions since it can undergo nucleophilic attack at the formamide group, leading to the deformylated diamino product compound and formic acid. Further nucleophilic attack on the imidiazole ring followed by deformylation would give polar nonchromophoric compounds. The latter reaction is probably very rapid in alkaline media (11–13), which accounts for the observation that the decomposition products of pentostatin at pH >11 were not detectable at 280 nm.

The data for the stability studies of pentostatin in aqueous acidic solutions (pH range of 1.0–3.5) at 37.0 ± 0.1°C to simulate gastric pH are presented in Table II. The rapid degradation of pentostatin in acidic pH values would preclude its use in non-enteric-coated oral dosage forms.

Formulation and iv Stability Studies. Pentostatin was formulated as a freeze-dried dosage form containing 10 mg of pentostatin, 50 mg of mannitol, and sodium hydroxide for pH adjustment. Kinetic studies suggested that pentostatin showed a maximum stability in the pH range of 7.0–9.0. To assess stability of reconstituted (with NS) lyophilized pentostatin prepared by BenVenue laboratories, the samples were further diluted to various concentrations of drug in either NS or D5W, in both PVC iv infusion bags and glass iv bottles. The containers were stored at ambient temperature (22–23°C) over a 48-hr period. Additionally, the drug concentration of the reconstituted lyophilized product without further dilution was monitored over a 72-hr period. The results are summarized in Table III and represent means ± SD for $n = 2$.

These data are in general agreement with the degradation of pentostatin projected from the pH–rate profile. That is, pentostatin has a reconstituted shelf life of >24 hr except when extensively diluted with D5W, where the shelf life can

be as short as ≈10–11 hr. The greater instability of pentostatin in D5W can be attributed to the lower pH in these solutions. Based on these findings, if longer-term storage in D5W is desired, it is suggested that the D5W solution be pH adjusted with sterile buffer to a neutral pH where the projected $t_{90\%}$ is >72 hr.

ACKNOWLEDGMENT

This work was supported by the National Cancer Institute, Contract NO1-CM-67912.

REFERENCES

1. R. P. Agarwal, T. Spector, and R. E. Parks, Jr. *Biochem. Pharmacol.* 26:359–367 (1977).
2. W. M. Shannon and F. M. Schabel, Jr. *Pharmacol. Ther.* 11:263–390 (1980).
3. P. W. K. Woo, H. W. Dion, S. M. Lange, L. F. Dahl, and L. J. Durham. *J. Heterocycl. Chem.* 11:641–643 (1974).
4. D. C. Baker, S. R. Putt, and H. D. Hollis Showalter. *J. Heterocycl. Chem.* 20:629–634 (1983).
5. E. Chan, S. R. Putt, H. D. Hollis Showalter, and D. C. Baker. *J. Org. Chem.* 47:3457–3464 (1982).
6. S. R. Putt and D. C. Baker. *J. Am. Chem. Soc.* 101:6127–6128 (1979).
7. E. H. Kraut, B. A. Bouroncle, and M. R. Grever. *Blood* 68:1119–1122 (1986).
8. A. Albert and E. D. Serjeant. In *Ionization Constant of Acids and Bases,* John Wiley & Sons, New York, 1962, pp. 9–22, 44–59.
9. B. D. Anderson, M. B. Wygant, T. X. Xiang, W. A. Waugh, and V. J. Stella. *Int. J. Pharm.* 45:27–37 (1988).
10. B. I. Perillo, B. Fernandez, and S. Lamdan. *J.C.S. Perkin* II:2068–2072 (1977).
11. E. R. Garrett and P. J. Mehta. *J. Am. Chem. Soc.* 94:8532–8541 (1972).
12. E. R. Garrett and P. J. Mehta. *J. Am. Chem. Soc.* 94:8542–8547 (1972).
13. J. L. York. *J. Org. Chem.* 46:2171–2173 (1981).
14. R. Th. Morrison and R. N. Boyd, *Organic Chemistry,* 3rd ed., Allyn and Bacon, 1973.
15. W. Pigman, *The Carbohydrates, Chemistry, Biochemistry, Physiology.* Academic Press, New York, 1957.
16. E. Breitmaier and W. Voelter. *Monographs in Modern Chemistry, Vol. 5,* Weinheim, Bergatr, 1974.
17. G. W. Kenner. In G. E. Wolsteholme and C. M. O'Connor (eds.), *The Chemistry and Biology of Purines,* Little, Brown, Boston, 1957, p. 312.
18. J. A. Zoltewicz, D. F. Clark, T. W. Sharpless, and G. Grahe. *J. Am. Chem. Soc.* 92:1741–1750 (1970).
19. J. A. Zoltewicz and D. F. Clark. *J. Org. Chem.* 37:1193–1197 (1972).
20. F. L. Boschke, W. Fresenius, J. F. K. Huber, E. Pungor, G. A. Rechnitz, W. Simon, and S. Th. West. *Tables of Spectral Data for Structure Determination of Organic Compounds,* Springer-Verlag, New York, 1983, P.H.-155.
21. R. H. DeWolfe and R. M. Roberts. *J. Am. Chem. Soc.* 75:2942–2947 (1953).
22. R. H. DeWolfe. In S. Patai (ed.), *The Chemistry of Amidines and Imidates,* John Wiley & Sons, 1975, Chap 8, pp. 349–384.